Available online at www.sciencedirect.com
SCIENCE DIRECT®

ELSEVIER

Polymer 45 (2004) 1555–1562

polymer

www.elsevier.com/locate/polymer

# Molecular mobility of CU(II)-containing liquid crystalline ionomers: dielectric relaxation and thermally stimulated depolarization currents

N.A. Nikonorova[a,*], T.I. Borisova[a], E.B. Barmatov[b], D.A. Pebalk[b], R.-D. Calleja[c]

[a]*Institute of Macromolecular Compounds of Russian Academy of Sciences, Bolshoy pr. 31, 199004 St Petersburg, Russian Federation*
[b]*Moscow State University, 119899 Moscow, Russian Federation*
[c]*Department of Applied Thermodynamics ETSII, Polytechnic University of Valencia, 4606 Valencia, Spain*

Received 25 June 2003; received in revised form 8 October 2003; accepted 8 December 2003

## Abstract

Molecular mobility of functionalized liquid crystalline (LC) copolymer (P1) containing mesogenic cyanobiphenyl groups and acrylic acid fragments (28%) as well as LC ionomers P2 (Cu 2.5() and P3 (Cu 7() with copper ions were studied by dielectric spectroscopy (DS) and by thermally stimulated depolarization current (TSDC) methods. For P1–P3, the frequency dependences of dielectric losses and temperature dependences of depolarization current were obtained and four relaxation processes $\gamma_1$, $\beta$, $\alpha$, and $\delta$ were found. For each of them a molecular mechanism was proposed. Moreover, for P1, P2, and P3, at high temperatures the TSDC global curves indicate the peak of depolarization current, which has no analogue in the dielectric spectrum. For P1 this peak is a $\rho$-process of low intensity. For P2 and P3 ionomers the intensity and temperature position of the high temperature peak increase as compared to those of P1. The mechanisms of the high temperatures peak for the P2 and P3 systems containing copper ions were attributed to the free space charge polarization and to the dipole polarization process of polymer chains included in ionic associates (multiplets). There is good correlation between the peak temperature positions obtained from the global TSDC spectrum at equivalent frequency and those obtained from DS.

*Keywords:* LC side-chain iononers; Dielectric spectroscopy; Thermally stimulated depolarization currents

## 1. Introduction

At the end of 20th century the evolution of research in the field of liquid crystalline (LC) polymers gave birth to various metal-containing macromolecular compounds capable of mesophase formation. The important reason for studying such systems is due to the fact that the incorporation of metal ions into ordered polymer matrix opens a way to novel generations of functional materials with a set of valuable properties: optical anisotropy, orientation in external fields, magnetic activity and etc [1–3]. In ion-containing LC polymers, the metal atoms play the role of counterions which compensate for negative charges of functional fragments bounded to polymer chains.

One of the important classes of metal-containing LC polymers is presented by the so-called LC ionomers that combine specific features of both LC polymers and amorphous ionomers [4–10]. This could be explained in the following way. The anisodiametric mesogenic groups of LC ionomers are able to form various LC phases: nematic, cholesteric (chiral nematic), and smectic. At the same time their charged groups are able to form ion aggregates (multiplets, clusters) that act as the points of noncovalent polymer chain crosslinking and provide specific morphology and properties of the usual statistical ionomers [11–14]. The main factors that control the phase behaviour and structure of LC ionomers are the concentration of metal ions, the polymer matrix structure, and the chemical nature of metal ions and charged groups.

Metal-containing side-chain LC ionomers are usually obtained on the basis of LC polymer with functional (for example, acidic) groups and mesogenic side groups [7,9,10]. It has already been shown that heavy (multi valent) metal atoms are able to interact with LC polymer not only as a result of simple electrostatic forces, but also through the formation of different types of inter- and intra-molecular complexes [15,16]. That is why it is very important to find

---

[*] Corresponding author. Tel.: +7-812-3288535; fax: +7-812-3286869.
*E-mail address:* nikon@imc.marco.ru (N.A. Nikonorova).

0032-3861/$ - see front matter © 2003 Elsevier Ltd. All rights reserved.
doi:10.1016/j.polymer.2003.12.049

out in what way such interactions influence the supramolecular organization of LC polymer and the molecular mobility of its elements.

Different modes of molecular mobility in polymers of varied classes, including thermotropic side-chain liquid crystalline polymers (SCLCPs), are being studied successfully by the classical method of dielectric spectroscopy (DS) [17–19]. The decoding of a dielectric spectrum allows us to identify the observed relaxation processes with the mobility of certain kinetic units bearing a polar group. The method of thermally stimulated depolarization currents (TSDC) is also used to investigate the molecular mobility of polymers [20–22].

The results obtained by TSDC and DS can be compared with each other because the phenomena studied in both methods are determined by the dynamic behavior of the macromolecules. The peaks displayed on the $\varepsilon^{\parallel} = \varphi(f)$ (DS) and $I = \varphi(T)$ (TSDC) plots are due to the orientational mobility of kinetic units containing a polar group. The temperature position of depolarization current peaks $T_m$ formally corresponds to the temperature position of the $\varepsilon^{\parallel}$ peaks observed at the equivalent frequency $f_e$ which is determined as

$$f_e = E_a r/(2\pi R T_m^2), \qquad (1)$$

where $E_a$ is activation energy of the relaxation process, $r$ the heating rate, $R$ the gas constant, $T_m$ the temperature of the depolarization current maximum. The equivalent frequency values are in the range of $10^{-2}$–$10^{-4}$ Hz [23].

In the current work we have investigated molecular order and mobility in the side-chain LC copolymer P1 and copper(II)-containing LC ionomers P2 and P3 for which the chemical structures are shown below:

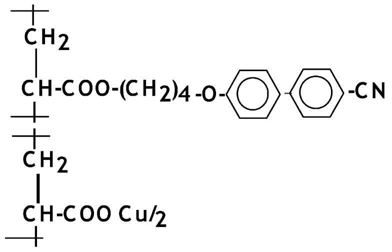

The aims of this work are as follows: (1) to study the molecular dynamics of the P1–P3 systems by DS and TSDC methods, (2) to identify the molecular mechanism of the observed processes, (3) to determine the influence of ion aggregate (multiplets) formation on molecular mobility of ionomer chains and side mesogenic groups.

## 2. Experimental part

In this work a functionalized LC polyacrylate P1 was obtained by free-radical copolymerization of 4-(cyanobiphenyl-4′-yloxy)-butyl acrylate (CB) (72%) with acrylic acid (AA) (28%) [24]. Then P1 (Cu = 0() was used as a polymer for obtaining LC Cu-containing ionomers: P2 (Cu = 2,5%) and P3 (Cu = 7%) [15,16]. For this purpose, a calculated amount of the freshly prepared solution of copper acetylacetonate in ethyl alcohol was added to the P1 copolymer solution in THF. For the P1–P3 polymers the phase and glass transition temperatures determined by DSC and $T_m$ (temperatures of $I_m$ on the main global TSDC curves in the range of 20–80 °C) are presented in the Table 1.

Dielectric measurements were performed with a three terminal plane condenser and a capacitance apparatus a DEA-2970. The samples were sandwiched between gold electrodes at 70 °C (in the rubbery state). The diameter of the potential electrode was 5 mm.

TSDC experiments were made on a TSC-RMA (Thermhold) spectrometer. The samples were polymer pellets of 0.34 mm thick and with a surface area of 76 mm$^2$. The global TSDC curves were obtained in the following conditions: the sample was polarized by a dc electric field ($U_p$ = 50–300 V/mm) at a polarization temperature ($T_p$ = 40–60 °C) and cooled down to the lowest temperature $T_0$. The field was then removed, the sample was connected to an electrometer and heated at a constant rate r to the final temperature $T_f$, and the depolarization current $I$ was recorded as a function of temperature $T$.

## 3. Results and discussion

### 3.1. Low temperatures

The global curves for the P1–P3 samples at low temperatures show that the temperature dependences of depolarization current $I = \varphi(T)$ have two overlapping peaks (Fig. 1). The first of them, a pronounced peak, is located near −112 °C, whereas the second, a less intensive peak observed as a shoulder, is located close to −130 °C.

It is known that dielectric investigation in the sub-glass state for a great number of SCLCPs revealed three local relaxation processes, β, $\gamma_1$ and $\gamma_2$, at successively decreasing temperatures [17–19,25–29]. Successive changes in the chemical structures of side-chain LC polymers allow us to relate the β, $\gamma_1$, and $\gamma_2$ processes to the rotational mobility of the mesogen about its long axis, to the mobility of the

Table 1
Phase behavior and temperature (in °C) of the depolarization current maximum $T_m$ of α, δ and ρ-processes observed on global TSDC spectrum for LC copolymer P1 and ionomers P2, P3

| Sample | Phase behavior (°C) | $T_{m\alpha}$ | $T_{m\delta}$ | $T_{m\rho}$ | $T_g$ [b] |
|---|---|---|---|---|---|
| P1 | G[a] 52 SmA 108 N 110 I | 48 | 56 | 65 | 50 |
| P2 | G[a] 49 SmA 108 I | 47 | 54 | 74 | |
| P3 | G[a] 48 SmA 104 I | 45 | 52 | 76 | 46 |

[a] Glass transition temperature obtaining by DSC data.

[b] Glass transition temperature obtaining by DS at 1 s.

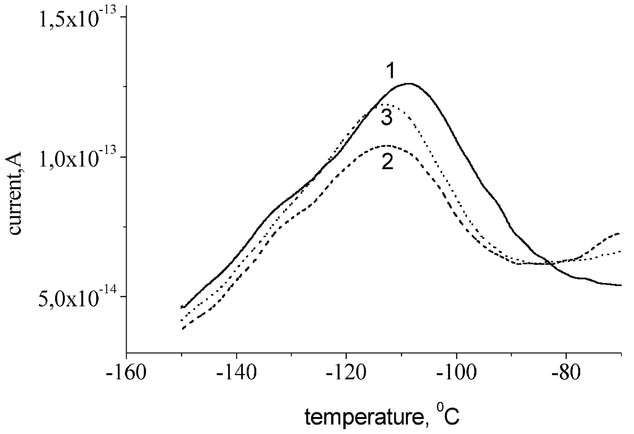

Fig. 1. Global TSDC spectrum for P1(1), P2(2), and P3(3) in the range of the $\gamma_1$ and $\beta$ processes.

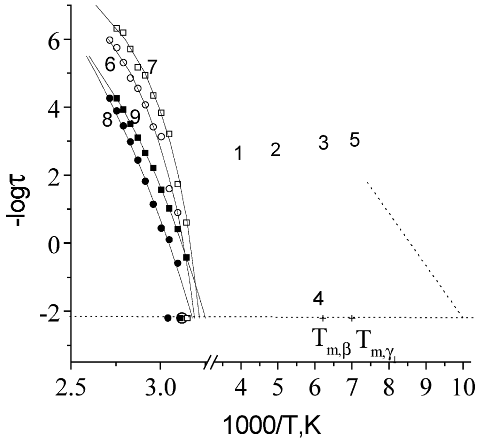

Fig. 2. Dependences of $-\log \tau$ on inverse temperature in the range of the $\alpha$ (6,7) and $-\delta$ (8,9) processes for P1 (6,8) and P3 (7,9) and in the range of the sub-glass processes (1–5) for PM-5-CAB (curves 1, 2) [25,27], PM-5-PhB (curves 1–3) [28,30], and for P1 with 38( AA (curves 4, 5) [31]; the points at $-\log \tau = -2.2$ are the $T_m$ values obtained from the global curves.

methylene spacers, and to the motion of terminal polar groups of the mesogen, respectively.

In the range of the $\beta$ process the relaxation times for SCLCPs of different structures are very close to each other. The activation energies for the $\beta$ process range from 48 to 75 kJ/mol [17–19,25,27,29]. In the case of the $\gamma_1$ process, the relaxation times for thermotropic LC side-chain PA-*n*-CAB and PA-*n*-PhB polyacrylates and PMA-*n*-CAB and PMA-*n*-PhB polymethacrylates (*n* is a number of methylene groups in the spacer, CAB and PhB are cyanazobenzene and phenynbenzoate side mesogen groups, respectively) decrease with methylene spacer length [26–29]. Thus, for PA-11-CAB and PMA-11-CAB, the difference in relaxation times between the $\beta$ and the $\gamma_1$ processes is about three order of magnitude. For PMA-5-CAB, PMA-5-Phb, and PA-5-CAB, it is still possible to observe two strongly overlapping $\beta$ and $\gamma_1$ processes which differ from each other in relaxation time by not more than half an order [26–28]. In the case of PA-3-CAB and PMA-3-CAB, the $\beta$ and the $\gamma_1$ processes merge, and only one relaxation process ($\beta/\gamma_1$) takes place [27]. For the $\gamma_1$ process, activation energies are in the range of 33–45 kJ/mol. As for the most rapid dielectric $\gamma_2$ process, its activation energies are about 21–33 kJ/mol [17–19,29,30].

To identify the molecular mechanisms of relaxation processes observed on the global curves (Fig. 1), it is of interesting to compare the TSDC and dielectric behavior of SCLCPs with similar structures at the sub-glass state. Fig. 2 shows the $-\log \tau = \varphi(1/T)$ plots for PMA-5-CAB and PMA-5-PhB in the ranges of the $\beta$, $\gamma_1$, and $\gamma_2$ processes, curves 1, 2, and 3, respectively [25,27,28,30]. The $\beta$, $\gamma_1$, and $\gamma_2$, processes are the local processes relaxation of dipole polarization. Usually, the temperature dependences of relaxation time for the local processes could be approximated by a linear Arrhenius curve. Postulating that the equivalent TSDC frequency is equal to $10^{-3}$ Hz ($\log \tau_m = 2.2$) [21,23], the linear plots in Fig. 2 (curves 1–3) were extrapolated to $-\log \tau_m = -2.2$. The extrapolated temperatures for the $\gamma_1$ and $\beta$ processes obtained in this way are close to $T_m$ observed on the global TSDC curves. This means that the peaks on the global curves in Fig. 1 are caused by the $\gamma_1$ and the $\beta$ processes. (For the $\gamma_2$ process, the extrapolated temperature equal to −176 °C is outside of the experimental range of the global curve).

Fig. 2 also shows the $-\log \tau_m = \varphi(1/T)$ plots in the sub-glass state for P1 with 38( of AA (curves 4, 5) [31]. One can see that curve 4 is placed between curve 1 and 2 corresponding to the $\beta$ and the $\gamma_1$ processes, respectively. This means that only a single $\beta/\gamma_1$ process is observed for P1. This fact is not surprising because the spacer length for P1 is small (it includes four methylene groups). In contrast to the dielectric results, the global TSDC curves show that at low temperatures it is possible to observe not a single $\beta/\gamma_1$ process but both the $\beta$ and the $\gamma_1$ processes (Fig. 1). This is due to the better resolution of TSDC curves in comparison to DS ones.

As for the lowest temperature relaxation process for P1 (38% of AA), it could be attributed to the rotational mobility of the terminal –OOH groups in the AA fragments because relaxation times of this process (curve 5) coincides satisfactorily with those for the $\gamma_2$ process (curve 3).

The comparison of curves 1–3 in Fig. 1 shows that in the sub-glass state the TSDC spectrum for the P1 copolymer has no principal difference with that for the P2 and P3 Cu-containing ionomers. This means that formation of multiplet structures does not influence the local relaxation processes at low temperatures.

### 3.2. High temperatures

Near $T_g$, the dielectric data for thermotropic SCLCPs show two overlapping cooperative processes, the $\alpha$ and the $\delta$ processes [17–19,30–35]. According to the theory [17,18, 34], the dipole correlation function can be expressed in terms of four dipole contributions (00, 01, 11, and 10 modes). The frequencies of these modes are related to the nature of the motion and they could be ranked as:

$$f_{00} < f_{01} \leq f_{11} \leq f_{10}$$

The δ process located at higher temperatures (low frequencies) corresponds to one of these modes (the 00 mode) and reflects the mesogen group reorientation about its short axis (relaxation of longitudinal component of dipole moment of mesogen $\mu_{\|}$). The α process is associated with the main-chain motion and with reorientation about the long axis of mesogen (relaxation of transverse component of dipole moment of mesogen $\mu_{\perp}$). The α process could be considered as a mixture of 01, 10, and 11 modes which occur at similar frequencies. This multiplicity of motions is possibly responsible for the broad relaxation times distribution for the α process. In practice, for SCLCPs it is impossible to divide into separate modes the dielectric dependences in the range of the α process.

The reason for the appearance of the δ process in thermotropic side-chain polymers follows from the peculiarity of the chemical constitution of this class of polymers. The fact is that mesogenic groups in SCLCPs are bonded to the macromolecule only at one end, and the flexible spacers provide the motion of mesogens, which is rather independent of the main chains motion.

### 3.2.1. Dielectric relaxation results

For P1 and P3, the frequency dependences of loss factor $\varepsilon^{\|}$ were obtained in the frequency and temperature ranges $10^{-1}$–$10^{5}$ Hz and + 20– + 95 °C, respectively. The temperature range included the glassy and the liquid-crystalline states. The shape of these dependences is similar for P1 and P3 samples. As an example, Fig. 3 shows the $\varepsilon^{\|} = \varphi(f)$ plots for P3 at several temperatures. One can see that the observed process of relaxation of dipole polarization is rather broad. According to the above considerations, this process could be presented as a superposition of two overlapping relaxation processes which will be designated as the α, and the δ processes in the order of increasing temperature.

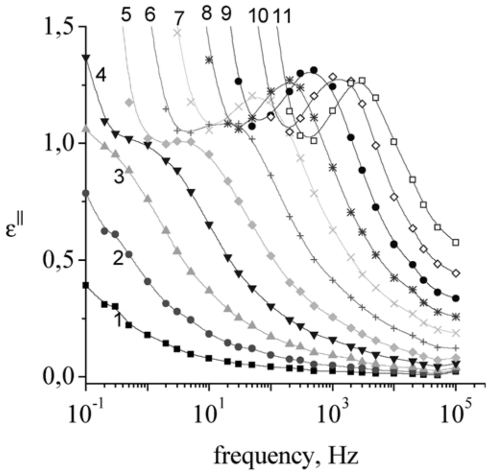

Fig. 3. Frequency dependences of dielectric loss factor $\varepsilon^{\|}$ for P3 at: 40 (1), 45 (2), 50 (3), 55 (4), 60 (5), 65 (6), 70 (7), 75 (8), 80 (9), 85 (10), and 90 °C (11).

To determine the kinetic parameters of the observed relaxation processes, the frequency dependences of $\varepsilon^{\|}$ were described by a sum of two empirical Havriliak–Negami (HN) functions and the conductivity contribution [36,37]:

$$\varepsilon^{\|} = \frac{\sigma_0}{\varepsilon_0}\frac{a}{\omega^s} - \sum_{k=1}^{2} \mathrm{Im}\left[\frac{\Delta\varepsilon_k}{(1+(\mathrm{i}\omega\tau HN_k)^{\alpha_k})^{\beta_k}}\right] \tag{2}$$

The first term in Eq. (2) is caused by translation diffusion of mobile charge carriers, where $\varepsilon_0$ is the vacuum permittivity, $\sigma_0$ is the dc conductivity, $s \leq 1$, $a$ is a factor having the dimensionality $[a] = [\mathrm{Hz}]^{s-1}$, $\omega = 2\pi f$, and $f$ is the frequency of the ac electric field. The index $k$ refers to the α or to the δ process; Δε is the dielectric relaxation strength, and α and β are fit parameters describing the broadening and the asymmetry of relaxation time distribution, respectively.

As an example, Fig. 4 shows for P1(a) and P3(b) the

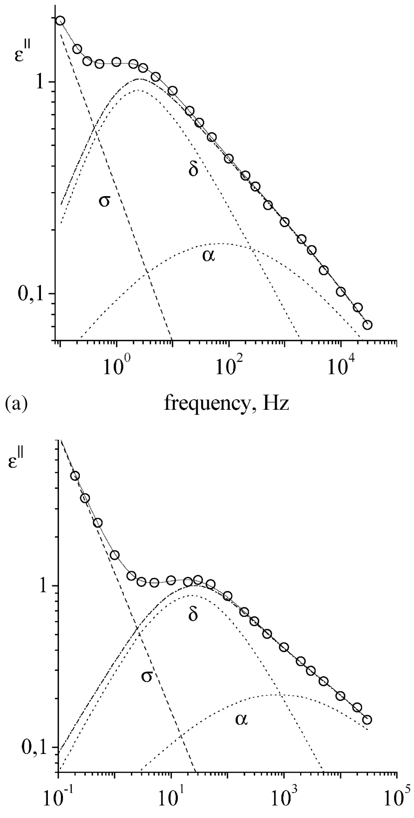

Fig. 4. Frequency dependence of $\varepsilon^{\|}$ for P1(a) and P3(b) at 65 °C. The open circles are the experimental points. The solid line is the best fit given by the superposition of a conductivity term $\sigma$ (dashed line) and contributions due to the α and δ processes (dotted lines) calculated according to Eq. (2). The dashed-dotted line is the contribution due to dipole relaxation (fit curve without the conductivity term). The fitting parameters for P1 are: $\sigma = 1.05\times10^{-11}$ 1/Ω cm, $s = 0.73$, $\Delta\varepsilon_\alpha = 1.15$, $\alpha_\alpha = 0.37$, $\beta_\alpha = 0.33$, $\log\tau_\alpha = -3.42$; $\Delta\varepsilon_\delta = 3.13$, $\alpha_\delta = 0.8$, $\beta_\delta = 0.69$, $\log\tau_\delta = -1.14$ and for P3 are: $\sigma = 5.1\times10^{-11}$ 1/Ω cm, $s = 0.87$, $\Delta\varepsilon_\alpha = 0.78$, $\alpha_\alpha = 0.4$, $\beta_\alpha = 0.20$, $\log\tau_\alpha = -4.34$; $\Delta\varepsilon_\delta = 3.83$, $\alpha_\delta = 0.68$, $\beta_\delta = 1$, $\log\tau_\delta = -2.21$.

$\varepsilon^{\|} = \varphi(f)$ dependences at 65 °C presented as a superposition of the α and the δ processes and the conductivity term, which were calculated in accordance to Eq. (2). For P1 and P3, the temperature dependences of relaxation time calculated from Eq. (2) in the range of the α and the δ processes are shown in Fig. 2 (curves 6–9). Apart from the fact that the α and δ processes are very close to each other their separation in accordance to Eq. (2) gives rather reliable results in the relaxation time values. The error does not exceed the symbols size in Fig. 2.

In thermotropic side-chains polymers the features of the α process corresponded to cooperative segmental motion of the main chains are similar to those observed in amorphous and semicrystalline conventional polymers: high activation energy, broad relaxation time distribution, close coincidence of $T_g$ obtained by DSC and by dielectric methods, and the temperature dependence of relaxation time. These dependences (the $-\log \tau_m = \varphi(1/T)$ plots) for SCLCPs, just as for polymers of other classes, in the range of the α transition in a wide temperature range are well described by the empirical Vogel–Tammann–Fulcher–Hesse (VTFH) equation [17,18,30,37,38]:

$$f_m = A \exp\left(-\frac{B}{T - T_0}\right), \tag{3}$$

where $A$, $B$, and $T_0$ are the temperature-independent empirical parameters. $A$ is a high-temperature limited relaxation rate, $B$ is the activation parameter, and $T_0$, called the Vogel temperature or the ideal glass transition temperature, is usually a few tens of degrees below $T_g$.

The temperature dependences of relaxation times for P1 and P3 in the range of the α process were fitted by Eq. (3). The fit parameters for P1 are: $\log A = 10.45$, $B = 381$ K, and $T_0 = 284$ K, whereas those for P3 are: $\log A = 10.1$, $B = 282$ K, and $T_0 = 288$ K.

To determine the $T_g$ from dielectric data, the VTFH dependence in the range of the α process should be extrapolated to 1 s or to $10^3$ s, i.e. to $\log f_m = 0$ or $\log f_m = -3$ ($-\log \tau_m = 0.8$ or $-\log \tau_m = -2.2$). For P1 and P3, the extrapolation of curves 6 and 8 in Fig. 2 gives the $T_g$ values equal to 50 (at 1 s) or 41 °C (at $10^3$ s) and 46 (at 1 s) or 38 °C (at $10^3$ s), respectively. The $T_g$ values obtained from dielectric data at relaxation time 1 s are lower by 2 °C than those determined by DSC (Table 1). This difference between $T_g$ values obtained by the two methods is within the experimental error.

The question is why the glass transition temperature for P1 is higher than that for the metal-containing ionomers P2 and P3? The following explanation could be suggested. The macromolecule of copolymer P1 consists of the CB and AA fragments. Due to the hydrogen bonds, the main chains of polyacrylic acid (PAA) become very rigid, therefore it does not pass into the rubbery state. Hence, it is impossible to determine directly the $T_g$ of PAA. Using different methods, the glass transition temperatures of PAA (estimated by extrapolation) were obtained in the range of 80–166 °C [39]. The $T_g$ of homopolymer CB is 43 °C [24]. For the P1 copolymer the presence of rigid AA fragments (28%) in the polymer main chain increases $T_g$ to 52 °C. For the P2 and P3 ionomers, the incorporation of Cu ions (2.5 or 7%) into the copolymer P1 destroys the hydrogen bonds. This leads to some decrease of the $T_g$ values for P2 and P3 in comparison to P1.

The temperature dependence of relaxation time for the δ process occurring in the LC state can be described by the Arrhenius [33,35,40] or by the VTFH dependence [30,41]. In the present work the $-\log \tau = \varphi(1/T)$ dependences were described for P1 and P3 by Eq. (3) with the fit parameters: $\log A = 16.4$, $B = 1892$ K, $T_0 = 213$ K and $\log A = 13.4$, $B = 1162$ K, $T_0 = 232$ K, respectively. The transition temperatures of the δ process for P1 and P3 determined by the extrapolation of the VTFH fit curves are 61 (at 1 s) or 41 °C (at $10^3$ s) and 53 (at 1 s) or 35 °C (at $10^3$ s), respectively.

The extrapolated temperatures for the δ process at relaxation time 1 s are higher than those for the α process by about 10 °C. At relaxation time $10^3$ s the temperatures transitions for the α and the δ processes are close to each other. This fact can be explained by the following consideration. In side-chain LC polymers, the δ process (in $\varepsilon^{\|} = \varphi(T)$ dependences in the range of radio frequences) is usually observed in the rubbery state at temperature 5–30 °C higher than that of the α process [17–19,30,31,33,35,40,41]. This follows from the fact that the reorientation of mesogens about the short axis requires a large free volume and takes place only in conditions of segmental mobility of the backbone, when the modes associated to the mesogenic group motion are activated. It was shown that the activation energy values for the α process are 20–50% higher than those for the δ process [30,31,33–38,40–42]. Hence, with decreasing frequency these processes become closer to each other, and the situation when the δ process will formally precede the α process could be achieved.

For the P1, P2, and P3 copolymers, in 20–90 °C temperature range, in addition to dielectric dependences, the temperature dependences of depolarization current $I = \varphi(T)$ were also obtained (Fig. 5(a)–(c), respectively). These figures show that near $T_g$, two depolarization current peaks are observed.

The peaks on the global TSDC curves could be caused by several reasons: relaxation of dipole polarization, ionic vacancy migration, drift of electrons or holes, and excess charge injection from electrodes [43]. For decoding the TSDC spectrum, it is important to make a distinction between dipole relaxation and free charge processes. Several procedures for understanding the nature of the observed peaks have been proposed [21,44]. The simplest way is to obtain a series of global curves with different polarizing electric fields $U_p$. If the intensity of depolarization current $I_m$ shows a linear dependence on $U_p$, this fact is often considered as an indication of the dipolar nature of the corresponding relaxation mechanisms. For the P1–P3

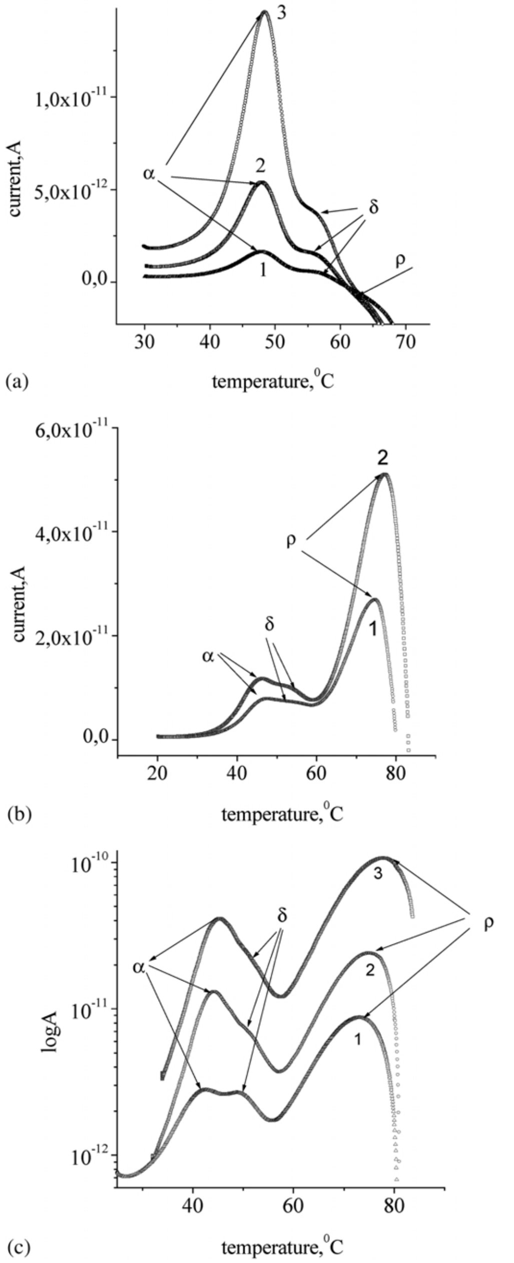

Fig. 5. Global TSDC spectrum in the range of the α, δ, and ρ processes for P1(a) at $T_p = 50$ °C and $U_p = 50(1)$, 100(2), and 200(3) V/mm, for P2(b) at $T_p = 60$ °C and $U_p = 50(1)$ and 100(2) V/mm, and for P3(c) at $T_p = 60$ °C and $U_p = 50(1)$, 100(2), and 300(3) V/mm.

systems studied here, the $I_m = \varphi(U_p)$ dependences are linear for both peaks near $T_g$ (Fig. 6). This means that these peaks are caused by dipole polarization.

For the P1, P2, and P3 samples, the temperatures of the first peak on the global TSDC curve in Fig. 5 are observed at 48, 47 and 45 °C, respectively. These temperatures (as in the case of the dielectric method) are lower by several degrees than the glass transition temperatures determined by DSC (Table 1). One can suppose that the first peak could be ascribed to the α process.

The second peak on the global curves is located at 56, 54, and 52 °C for P1, P2, and P3, respectively (Fig. 5). One can suppose that the second $I_m$ peak in Fig. 5, which is higher than the first peak by 7–8 °C, could be attributed to the δ peak. The same difference between the temperature positions of the α and δ processes was observed in dielectric measurements (Fig. 2). At the same time, as shown above, this difference diminishes with relaxation time increasing and achieves the negative values at relaxation times $10^3$ s. In the range of the δ process, the approximation of the $-\log \tau_m = \varphi(1/T)$, plots to very low frequences by VTHF equation is probably not quite valid. This fact requires additional experimental data to be obtained for the model systems. We plan to consider this phenomenon in future.

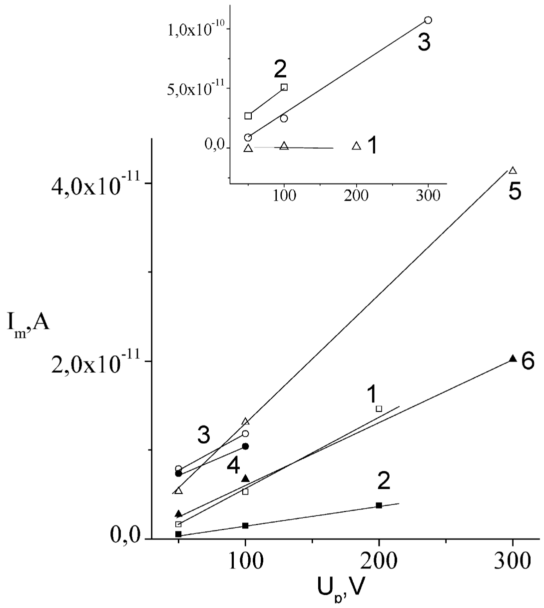

Fig. 6. Dependences of $I_m$ on $U_p$ for P1(1,2), P2(3,4), and P3(5,6) in the range of the α (1,3,5) and δ (2,4,6) processes; insert shows the same dependences for the high temperature TSDC peak for P1(1), P2(2), and P3(3).

Fig. 5 also show that the α depolarization peak is more prominent than the δ peak. The opposite situation was observed for dielectric measurements when the α process is observed as a shoulder on the well pronounced δ relaxation (Fig. 4). Besides this fact, there is another indication of the qualitative difference between the results obtained by dielectric and TSDC methods. Thus, near $T_g$, for SCLCPs with very different structures of mesogens and the main chains, the dielectric data show only two processes. In contrast to dielectric data, near $T_g$, the TSDC global spectrum for thermotropic side-chain polysiloxanes with phenylbenzoate mesogens having both $\mu_\perp$ and $\mu_\parallel$ components of the dipole moment of mesogen showed three peaks [20,21]. It was suggested that the first peak is related to the glass transition, the second one to the relaxation of $\mu_\perp$, and the third one to the relaxation of $\mu_\parallel$ of the mesogen dipole moment. In the case of polysiloxanes with cyanobiphenyl mesogens having only the $\mu_\parallel$ component of the mesogen dipole moment, near $T_g$, only two peaks in the

$I = \varphi(T)$ dependence were observed [45,46]. These peaks were attributed to the main chain motion and to the reorientation of mesogen about of its short axis, i.e. to the δ process. The copolymers studied here have cyanobiphenyl mesogenic side groups. As a result, only the δ process above $T_g$ was observed on the global curves (Fig. 5).

One can see that for the P1, P2, and P3 systems, on the global TSDC curve there is a third high temperature peak in addition to the α and δ peaks (Fig. 5). This process has no analogues on dielectric and DSC dependences. For usual amorphous and semicrystalline polymers, the highest temperature peak on the global curves, generally called the ρ-peak, is usually related to the motion of excess free charges limited in space by drift and diffusion.

For the P1 copolymer this peak occurs at 65 °C and has negative values of $I_m$ equal to $-8.5 \times 10^{-13}$ A (Fig. 5(a)). Its intensity and $T_m$ values are independent of polarization voltage in the range of 50–200 V (insert in Fig. 6, curve 1). The features of this peak for P1 indicate that it is the typical ρ-peak caused by free space charge polarization and by injection of charges from the electrodes [43,47–49].

One can see that for the P2 and P3 Cu-containing ionomers the depolarization current values for the third peak on the global curve decrease abruptly passing through zero and at 80 °C achieve negative values equal to $-1 \times 10^{-11}$ A (Fig. 5(b) and (c)). This situation is typical for the ρ-peak caused by free space charge polarization.

On the other hand, for the Cu-containing ionomers, the incorporation of copper ions changes the character of the high temperature peak which has certain new specific features in comparison with those for P1. First, in the case of the P2 and P3 ionomers, the highest temperature peak appears at 74–77 °C (Fig. 5(b) and (c)), i.e. about 10 °C higher than that for P1. Second, the intensity of this peak for P2 and P3 increases in comparison with the $I_m$ values for P1 and achieves the values in 2–5 times higher than that of the α and the δ processes. Third, the most important thing is that the intensity of the high temperature TSDC peak increases with $U_p$. For the P3 ionomer studied here the $I_m$ values at $U_p = 50$, 100, and 300 V are equal to $8.7 \times 10^{-12}$, $2.5 \times 10^{-11}$, and $1.1 \times 10^{-10}$ A, respectively (insert in Fig. 6, curve 3). For the P2 ionomer, the $I_m$ values of the high temperature peak also increase with $U_p$ (insert in Fig. 6, curve 2). As written above, the intensity increasing of the TSDC peak with the $U_p$ values could be related with a dipolar contribution in the highest temperature peak for the Cu-containing ionomers.

It is evident that the peak on the global TSDC plots following the δ process is related to the presence of ionic multiplet structures in P2 and P3. In a similar manner, in Ref. [50] it has been suggested that for segmented polyurethane ionomers the highest temperature peak on the global TSDC curve reflects the properties of ionic aggregates (multiplets). At the same time, the space charge polarization and injection of charges from the electrodes may also contribute to the considered peak. It is most likely that for the investigated here LC ionomers the highest peak on the global TSDC curves includes both dipole origin and free charge components.

## 4. Conclusions

This work is the first attempt to study side-chain LC ionomers by TSDC and DS methods. For the ionogenic and nonionogenic systems studied here, it was shown that the local β and $\gamma_1$ and the cooperative α and δ processes have no essential distinctions in dielectric and TSDC behaviour. However, an important distinction is observed for the highest temperature peak on the global TSDC curve. This peak for the Cu-containing ionomers testifies the features of the ρ-peak and of the dipole polarization process caused by presence of ionic multiplet structures. To understand the molecular mechanisms of the observed peaks, we must have more extensive experimental results. In future we plan to perform the combined TSDC and DS investigation of LC ionomers containing ions of different charges and concentrations. Dielectric and TSDC methods giving different details of the observed relaxation processes, allow us to present the overall picture of molecular mobility in the systems under investigation. These two methods revealing the differences and similarities of the results could be considered as complementary to each other.

## Acknowledgements

This research was supported by RFBR (Grant 01-03-32943, 02-03-06219), INTAS YSF-01/1-90, and by grant of Comunidad Valenciana (resolution of CTT from 17.06.02)

## References

[1] Oriol L, Pinol M, Serrano JL. Prog Polym Sci 1997;22:873–911.
[2] Tantrawong S, Styring P. Liq Cryst 1997;22(1):17–22.
[3] Kaliayppan T, Kannan P. Prog Polym Sci 2000;22:343–7.
[4] Wiesemann A, Zentel R, Pakula T. Polymer 1992;33(24):5315–20.
[5] Brehmer M, Wiesemann A, Wischerhoff E, Zentel R. Mol Cryst Liq Cryst 1994;254:405–16.
[6] Wilbert G, Zentel R. Macromol Symp 1997;117:229–32.
[7] Lei H, Zhao Y. Polym Bull 1993;31:645–9.
[8] Zhao Y, Lei H. Macromolecules 1994;27(6):4525–9.
[9] Barmatov EB, Pebalk DA, Barmatova MV, Shibaev VP. Macromol Rapid Commun 2000;21:369–74.
[10] Barmatov EB, Pebalk DA, Barmatova MV, Shibaev VP. J Polym Sci Part A: Polym Chem 2001;39:3953–9.
[11] Eisenberg RA, King M. Ion containing polymers. New York: Haisted-Wiley; 1975.
[12] MacKnight WJ, Earnest TRJ. Polym Sci: Macromol Rev 1981;16: 41–122.
[13] Eisenberg RA, Hird B, Moore RB. Macromolecules 1990;23: 4098–107.

[14] Salamone JC, editor. Concise polymeric material encyclopedia. Boca Raton: CRC Press; 1999. p. 711–21.

[15] Barmatov EB, Prosvirin AV, Barmatova MV, Galyametdinov YuG, Haase W, Shibaev VP. Macromol Rapid Commun 2000;21(6):281–6.

[16] Barmatov EB, Pebalk DA, Barmatova MV, Shibaev VP. Polymer 2002;43:2875–80.

[17] Moscicki JK. In: Collyer AA, editor. Liquid crystal polymers: from structure to applications. London: Elsevier; 1992. p. 143–236. Chapter 4.

[18] Simon GP. In: Runt JP, Fitzgerald JJ, editors. Dielectric spectroscopy of polymeric materials. ACS series, Washington, DC: ACS; 1997. p. 329–78. Chapter 12.

[19] Zentel R, Strobl GR, Ringsdorf H. Macromolecules 1985;18(5): 960–5.

[20] Mura-Ramos JJ, Mano JF, Lacey D, Nestor G. J Polym Sci: Part B: Polym Phys 1996;34:2067–75.

[21] Mano JF, Correia NT, Moura-Ramos JJ, Andrews SR, Williams G. Liq Cryst 1996;20(2):201–17.

[22] Sauer BB, Mura-Ramos JJ. Polymer 1997;38(16):4065–9.

[23] Van Turnhout J. Thermally stimulated discharge of polymer electrets. Amsterdam: Elsevier Scientific; 1975.

[24] Barmatov EB, Pebalk DA, Barmatova MV, Shibaev VP. Liq Cryst 1997;23(3):447–51.

[25] Borisova TI, Nikonorova NA. Macromol Chem Phys 1998;199(10): 2147–52.

[26] Nikonorova NA, Borisova TI, Stakhanov AI, Kostromin SG, Shibaev VP. Polym Sci 1998;A40(1):24–9.

[27] Nikonorova NA, Borisova TI, Stakhanov AI, Shibaev VP. Mol Cryst Liq Cryst 1999;331:59–66.

[28] Nikonorova NA, Borisova TI, Shibaev VP, Barmatov EB, Georgoussis G, Pissis P. Macromol Chem Phys 2001;202(8):1313–8.

[29] Gedde UW, Lui F, Hellermark C, Hult A, Sahlem F, Boyd RH. JMS Pure Appl Chem 1996;A33(10):1555–63.

[30] Nikonorova NA, Borisova TI, Barmatov EB, Pissis P, Diaz-Calleja R. Polymer 2002;43:2229–38.

[31] Zhukov SV, Stuhn B, Borisova TI, Barmatov EB, Barmatova MV, Shibaev VP, Kremer F, Pissis P. Macromolecules 2001;34(11): 3615–25.

[32] Mijovic J, Jo-Wing Sy. Macromolecules 2001;33(26):9620–9.

[33] Nikonorova NA, Borisova TI, Shibaev VP. Macromol Chem Phys 2000;201(2):226–32.

[34] Araki K. Polym J 1990;22(6):546–50.

[35] Kresse H, Kostromin SG, Shibaev VP. Makromol Chem Rapid Commun 1981;3:509–13.

[36] Havriliak Jr S, Negami SJ. Polymer 1967;8(1):161–7.

[37] Merenga AS, Papadakis CM, Kremer F, Liu J, Yee AF. Macromolecules 2001;34(1):76–81.

[38] Kremer F, Valerien SU, Zentel R, Kapitza H. Macromolecules 1989; 22(10):4040–5.

[39] Illers K-H. Kolloid-Z 1963;190(1):16–34.

[40] Simon R, Coles HJ. J Polym Sci: Part B: Polym Phys 1989;27: 1823–36.

[41] Zhong ZZ, Schule DE, Smith SW, Gordon WL. Macromolecules 1993;26(24):6403–9.

[42] Nikonorova NA, Barmatov EB, Borisova TI, Shibaev VP. Polym Sci 1997;A39(4):404–11.

[43] Sessler GM. In: Sessler GM, editor. Physical principles of electrets. Berlin: Springer; 1980.

[44] Boersma A, van Turnhout J, Wubbenhorst M. Macromolecules 1998; 31(21):7453–60.

[45] Mano JF, Moura Ramos JJ, Fernandes A, Williams G. Polymer 1994; 35(24):5170–8.

[46] Mano JF, Correia NT, Moura Ramos JJ, Fernandes AJ. Polym Sci Polym Phys Ed 1995;33(1):269–75.

[47] Mudarra M, Belana J, Cañadas JC, Diego JA. Polymer 1999;40(13): 2659–65.

[48] Mudarra M, Belana J. Polymer 1997;38(23):5815–21.

[49] Liu S-F, Lee Y-D. J Polym Sci: Part B: Polym Phys 1995;33: 1333–41.

[50] Pissis P, Kyritsis A, Shilov VV. Solid State Ionics 1999;125:203–12.